

Article

## **Al<sub>2</sub>O<sub>3</sub> Disk Supported Si<sub>3</sub>N<sub>4</sub> Hydrogen Purification Membrane for Low Temperature Polymer Electrolyte Membrane Fuel Cells**

Xiaoteng Liu <sup>1,\*</sup>, Paul A. Christensen <sup>1</sup>, Stephen M. Kelly <sup>2</sup>, Vincent Rocher <sup>2</sup> and Keith Scott <sup>1</sup>

<sup>1</sup> School of Chemical Engineering and Advanced Materials, Merz Court, Newcastle University, Newcastle upon Tyne NE1 7RU, UK; E-Mails: paul.christensen@ncl.ac.uk (P.A.C.); k.scott@ncl.ac.uk (K.S.)

<sup>2</sup> Department of Chemistry, University of Hull, Cottingham Road, Hull HU6 7RX, UK; E-Mails: s.m.kelly@hull.ac.uk (S.M.K.); vincent.rocher@espci.org (V.R.)

\* Author to whom correspondence should be addressed; E-Mail: xiaoteng.liu@ncl.ac.uk; Tel.: +44-191-222-3070.

Received: 26 November 2013 / Accepted: 2 December 2013 / Published: 5 December 2013

---

**Abstract:** Reformate gas, a commonly employed fuel for polymer electrolyte membrane fuel cells (PEMFCs), contains carbon monoxide, which poisons Pt-containing anodes in such devices. A novel, low-cost mesoporous Si<sub>3</sub>N<sub>4</sub> selective gas separation material was tested as a hydrogen clean-up membrane to remove CO from simulated feed gas to single-cell PEMFC, employing Nafion as the polymer electrolyte membrane. Polarization and power density measurements and gas chromatography showed a clear effect of separating the CO from the gas mixture; the performance and durability of the fuel cell was thereby significantly improved.

**Keywords:** Al<sub>2</sub>O<sub>3</sub> disk supported Si<sub>3</sub>N<sub>4</sub> membrane; hydrogen purification; CO removal; fuel cells; Pt catalyst

---

### **1. Introduction**

The hydrogen-fuelled, proton-exchange membrane fuel cell is a promising power source because of its high power density, high-energy conversion efficiency and low emission level. However, it requires high-purity H<sub>2</sub> when operated at low temperatures, since impurities in the H<sub>2</sub> stream, such as CO, will

poison and therefore reduce the performance of Pt-based anodes. It has been reported that a CO concentration of 10 ppm and above will poison Pt [1,2]. A significant amount of research has been carried out to improve the CO tolerance by using advanced Pt alloy catalysts [3–6], or alternative membranes capable of operating at higher temperatures [7–11]. H<sub>2</sub> purifying devices can also be used to remove CO, but the use of such additional steps has a negative effect on the overall process in terms of cost and efficiency [12,13].

The low-cost mesoporous silicon nitride (Si<sub>3</sub>N<sub>4</sub>) employed in this study, has a high surface area ( $\geq 400 \text{ m}^2 \text{ g}^{-1}$ , determined using the Brunauer–Emmett–Teller (BET) method [14]) and a narrow pore-size distribution (20–60 Å) [14,15]. The small pore size and large polar surface area of silicon nitride renders it of possible interest with respect to application as a selective gas filter [16]. The polar nature of the surface sites on silicon nitride also gives rise to complicated physisorption and chemisorption reactions which may influence its gas separation properties [17,18]. A thin mesoporous Si<sub>3</sub>N<sub>4</sub> layer deposited on top of a microporous Al<sub>2</sub>O<sub>3</sub> disk support has shown high selective absorption of NO<sub>2</sub> [15], and also potential application in the separation of CO from reformat.

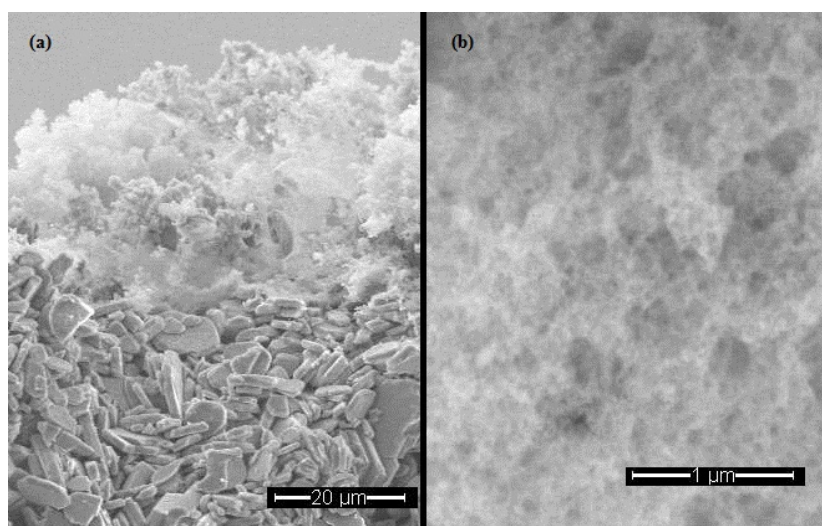
In the work reported in this paper, the Nafion membrane system was employed as the polymer electrolyte membrane (PEM) in the polymer electrolyte membrane fuel cells (PEMFCs) fuelled by a mix of CO and H<sub>2</sub> passing through a Si<sub>3</sub>N<sub>4</sub> membrane. Because it is clear to see the CO poisoning effect significantly reduces such fuel cell's performance which operates at low temperatures.

## 2. Results and Discussion

### 2.1. Scanning Electron Microscopy

Figure 1a shows a scanning electron micrograph (SEM) image ( $\times 1000$ ) of a cross-section of the Si<sub>3</sub>N<sub>4</sub> membrane supported on Al<sub>2</sub>O<sub>3</sub>. A reasonably uniform Si<sub>3</sub>N<sub>4</sub> appears on the top of the Al<sub>2</sub>O<sub>3</sub> disk. As can be seen in the figure, the thickness of the Si<sub>3</sub>N<sub>4</sub> layer was approximately 20  $\mu\text{m}$ . Figure 1b shows the Si<sub>3</sub>N<sub>4</sub> layer at higher magnification ( $\times 25,000$ ) and it appears from the figure that the Si<sub>3</sub>N<sub>4</sub> was highly porous and could possibly act as an effective absorbent for CO.

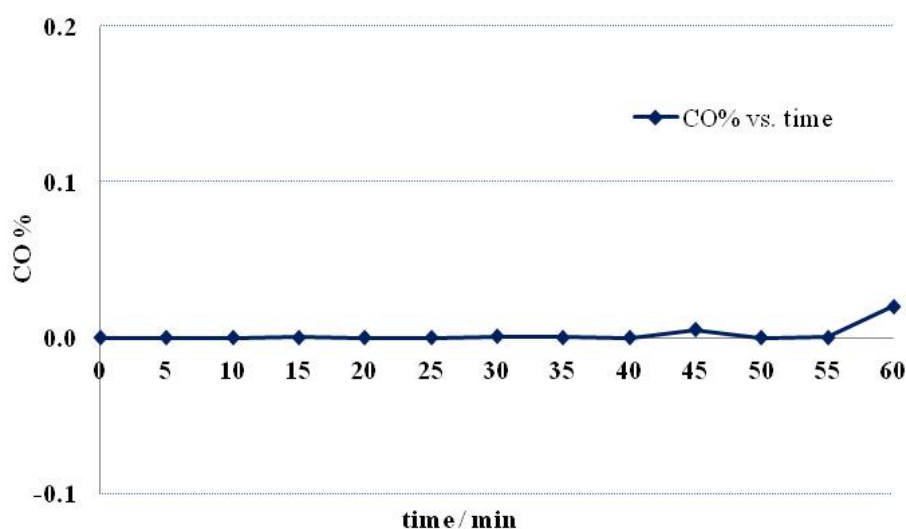
**Figure 1.** Scanning electron micrographs (SEMs) of the Si<sub>3</sub>N<sub>4</sub> membrane supported on Al<sub>2</sub>O<sub>3</sub>.



## 2.2. Gas Chromatography (GC)

The concentration of CO in H<sub>2</sub> in the exhaust from the filter H<sub>2</sub> (CO%) was calculated from the GC spectra. Figure 2 shows CO% as a function of operation time. As may be seen from the figure, CO was not detected in the outlet gas for the first 40 min; at longer times, the CO concentration slightly increased, suggesting the filter may allow a tiny amount of CO to pass through. The separation phenomenon might be via mixed chemisorption and physisorption functions, but it cannot be identified at this stage. The majority of CO was blocked by the membrane and discharged from the bypass outlet. The tiny amount of CO that passed through the membrane may have resulted from the layer of Si<sub>3</sub>N<sub>4</sub> being too thin. Increasing the amount of such material or packing it in a cartridge may be a possible solution.

**Figure 2.** The volumetric concentration of CO in the Si<sub>3</sub>N<sub>4</sub> membrane-filtered gas as a function of time.



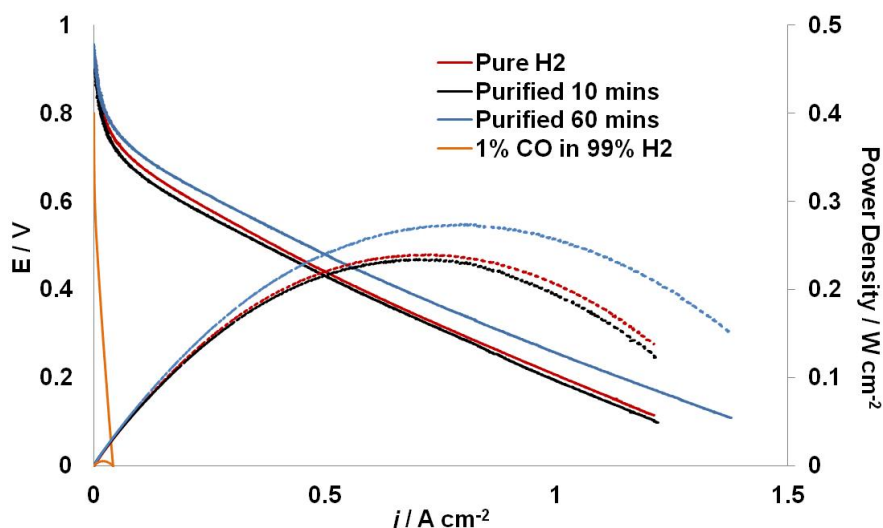
## 2.3. Fuel Cell Testing

Figure 3 shows the polarization curves and power density curves of the fuel cell. The fuel cell was operated for 60 min with the filtered gas as anode feeding gas, the forward sweep at 10 min and 60 min are shown. The curve obtained using pure H<sub>2</sub> as anode feeding gas in the same fuel cell is also included for comparison, as well as the curve obtained using 1% CO in 99% H<sub>2</sub> as anode feeding gas. The operating temperature of the PBI system was 80 °C.

With pure H<sub>2</sub>, a maximum power density of 0.29 W cm<sup>-2</sup> was achieved. The 1% CO in H<sub>2</sub> mixture filtered through the Si<sub>3</sub>N<sub>4</sub> membrane was then fed into the anode, replacing pure H<sub>2</sub>. The performance of the fuel cell was decreased with a maximum power density 0.24 W cm<sup>-2</sup>. As the bypass valve was slightly open, the flow rate after the membrane would be lower than 300 cm<sup>3</sup> min<sup>-1</sup>; presumably there was a small pressure drop too. This might be the reason for the lower fuel cell performance. However, after another 50 min operation, the fuel cell remained a similar performance with less than 0.01 W cm<sup>-2</sup> decreases in maximum power density. This is the evidence that the CO concentration of the filtered gas was lower than 10 ppm; the majority of CO was separated by the membrane. However, longer operation time will be needed to verify the separating function of the Si<sub>3</sub>N<sub>4</sub> membranes.

When the anode feeding gas switched to 1% CO in 99% H<sub>2</sub>, the fuel cell performance became affected from the very beginning, and it showed a complete CO poisoning effect to the anode catalyst.

**Figure 3.** Polarization (solid) and power density (dash) curves of the fuel cell. The blue curve fuel cell with pure H<sub>2</sub> as the anode feed. The red curves represent the fuel cell with anode feeding gas of filtered mixed gas at 10 min and the black curves represent the curves obtained at 60 min. The orange curves represent the fuel cell performance with anode feeding gas of 1% CO in 99% H<sub>2</sub>.



### 3. Experimental Section

#### 3.1. Si<sub>3</sub>N<sub>4</sub> Membrane

All chemicals were obtained from Sigma-Aldrich (Dorset, UK). The Al<sub>2</sub>O<sub>3</sub> disks, as the membrane support, were prepared from Al<sub>2</sub>O<sub>3</sub> powder using water as binder. The disks were then sintered at 1000 °C for 4 h. All procedures were performed under a protective nitrogen atmosphere using standard Schlenk techniques or in a nitrogen-filled glove box. The Si<sub>3</sub>N<sub>4</sub> membranes were prepared by dipping Al<sub>2</sub>O<sub>3</sub> support disks into a silicon di-imide sol followed by sintering [15,19]. Briefly, the silicon diimide sol was prepared by adding trifluoromethanesulfonic acid into a solution of TDSA in dry THF. The mixture was heated at 50 °C for 16 h then cool to room temperature. A solution of ammonia in cold THF was then added and the mixture left quiescent at room temperature for 18 h, then ammonia gas was bubbled through the solution for 10 min. After being left quiescent for 1 h, Al<sub>2</sub>O<sub>3</sub> support disks were dipped in the sol for 10 min and then dried under N<sub>2</sub> flow. After 30 min the disks were dipped again for another 10 min. The disks were dried under N<sub>2</sub> flow overnight and then pyrolyzed under NH<sub>3</sub> flow at 1000 °C for 2 h. The heating rate for the pyrolysis was 2 °C min<sup>-1</sup>. The disks so obtained were 1.6 cm in diameter, 0.1 cm in thickness, so that 4.5 cm<sup>2</sup> in total surface area. On average, 9 mg of dry Si<sub>3</sub>N<sub>4</sub> was deposited on each Al<sub>2</sub>O<sub>3</sub> disk.

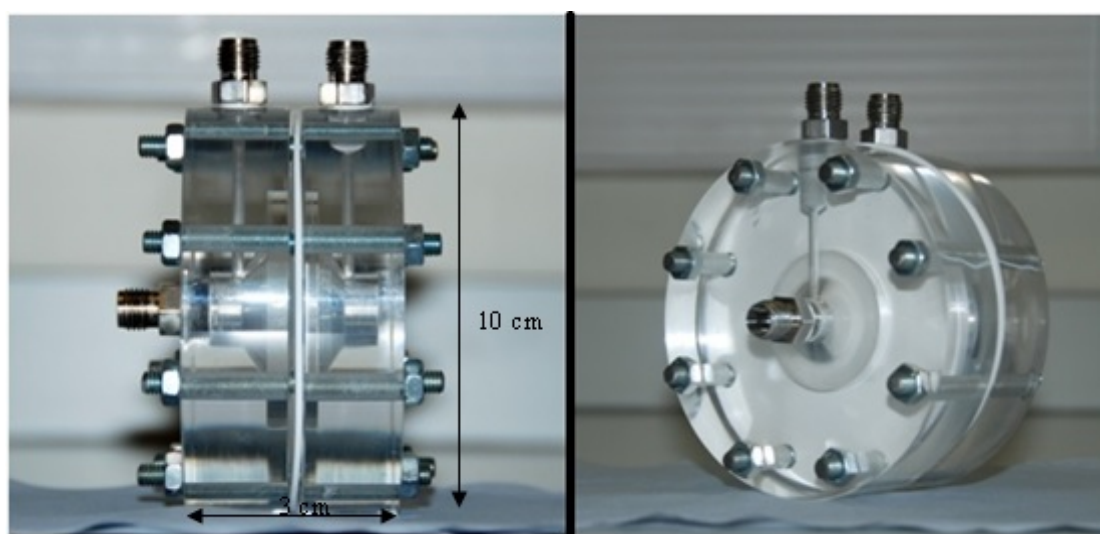
### 3.2. Scanning Electron Microscopy (SEM)

Scanning electron micrographs were obtained using a Philips XL30 ESEM-FEG SEM instrument. The  $\text{Si}_3\text{N}_4$  membrane was imaged without any additional coating. The membrane was dipped in liquid nitrogen and then broken using pliers to obtain a clean cross-section.

### 3.3. The Membrane Holder

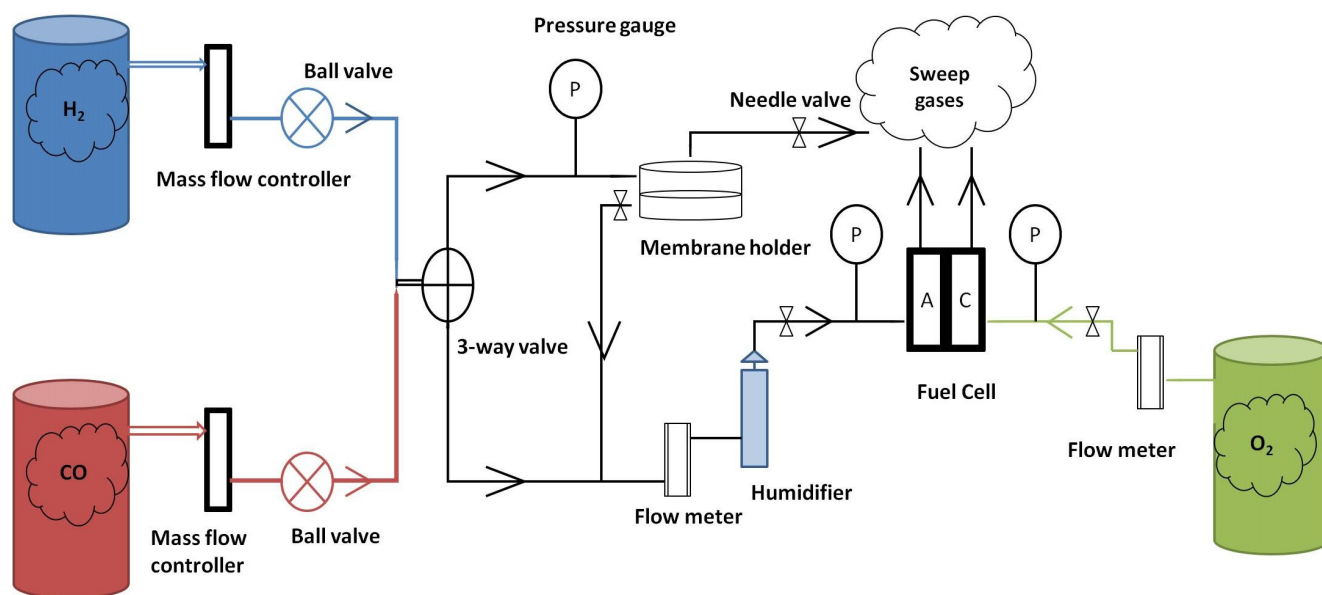
Figure 4 shows the holder cell for the  $\text{Si}_3\text{N}_4$  membranes. The cell allowed a mixture of various compositions of CO and  $\text{H}_2$  to flow through the membrane at rates up to  $300 \text{ cm}^3 \text{ min}^{-1}$ . The two chambers were made from poly(methyl methacrylate), and silicone rubber sheets were employed as gaskets to ensure a good seal between the holder and the  $\text{Si}_3\text{N}_4$  membrane. The edge of the membrane was covered by silicone rubber, and the effective area of the membrane was  $1.3 \text{ cm}^2$ . As it has been shown in Section 3.1 that each membrane has a surface area of  $4.5 \text{ cm}^2$ , assuming  $\text{Si}_3\text{N}_4$  was homogeneously deposited on the  $\text{Al}_2\text{O}_3$  disk, then 37.6% of the  $\text{Si}_3\text{N}_4$  was responsible for separating the CO.

**Figure 4.** The holder cell for the  $\text{Si}_3\text{N}_4$  membrane.



### 3.4. The Fuel Cell Test Rig

Figure 5 shows a schematic diagram of the fuel cell rig. The mass flow controllers were used to produce 1% CO in 99%  $\text{H}_2$  by volume for fuel cell test and gas chromatography (GC) test. The  $\text{CO} + \text{H}_2$  was fed to the  $\text{Si}_3\text{N}_4$  membrane at a flow rate of  $300 \text{ cm}^3 \text{ min}^{-1}$  and then humidified by passing through a humidifier with di-ionized water maintained at  $110 \text{ }^\circ\text{C}$  prior to entering the anode compartment of the PEMFC. The bypass needle valve (marked as A in Figure 5) was slightly open to allow filtered CO exhausting and keep neutral pressure before the membrane in the cell. The cathode feed gas was pure oxygen at a flow rate of  $300 \text{ mL min}^{-1}$ . The gas samples for GC were collected before entering the humidifier. All gasses were high purity (99.9%) and purchased from BOC Industrial Gases.

**Figure 5.** Schematic diagram of the fuel cell rig.

### 3.5. GC

One percent CO in 99% H<sub>2</sub> mixed gas at the rate of 300 mL min<sup>-1</sup> was fed to the Si<sub>3</sub>N<sub>4</sub> and then the exhaust gas samples were monitored using a SHIMADZU GC-8A Gas Chromatograph (Kyoto, Japan) fitted with a Molecular Sieve 5A column.

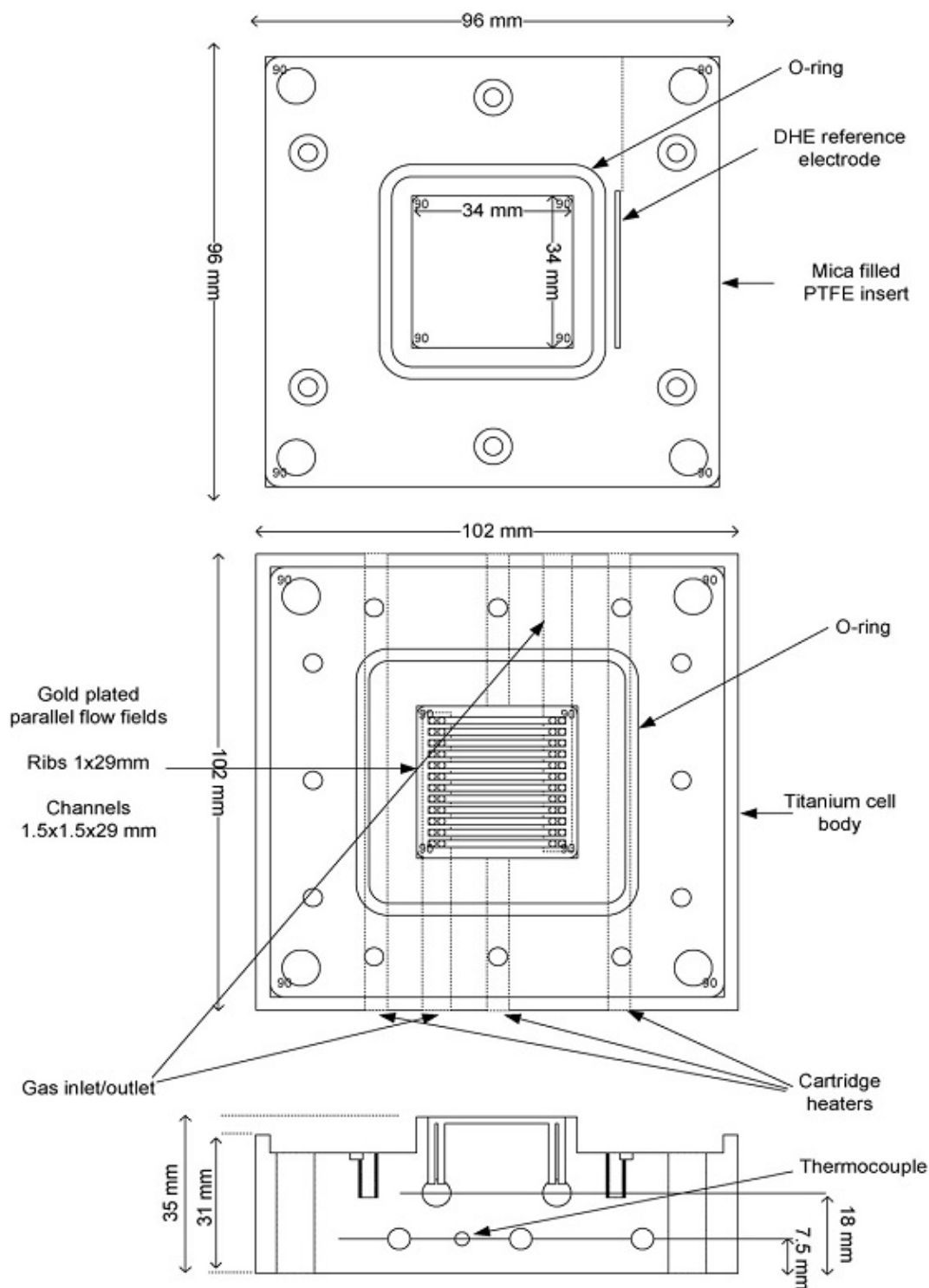
### 3.6. Fuel Cell and Membrane Electrolyte Assembly (MEA)

Details of the fuel cell employed may be found in previous papers [8,9,20]. Figure 6 shows a schematic diagram of the fuel cell. The cell body was made from titanium, the anode and cathode current collectors comprised 3.4 cm × 3.4 cm gold-plated Ti blocks, into which were cut parallel-flow fields to allow gases transport. Mica filled PTFE inserts were used to surround the flow fields and provide location for the O-ring seal and dynamic hydrogen electrodes (DHEs). The DHEs consisted of two platinum wires located on each side of the membrane outside the O-ring. Thermostatically controlled cartridge heaters (6 of 10 mm in diameter 100 mm in length, 150 W, RS, Northants, UK) were inserted into the Ti blocks to control the temperature. A 20 A potentiostat (Sycopel, UK) combined with a high impedance multi-channel data acquisition card (National Instruments, NI6010) was employed to carry out the electrochemical measurements. Polarisation curves were recorded during at a scan rate of 10 mV s<sup>-1</sup>.

The catalysts were purchased from Alfa Aesar. The anode was made from 20% Pt/C (VulcanXC-72) with a Pt loading of 0.2 mg cm<sup>-2</sup>. The cathode was made from 50% Pt/C (VulcanXC-72) with a Pt loading of 0.5 mg cm<sup>-2</sup>. 60% PTFE solution in di-ionized water (Sigma-Aldrich, Dorset, UK) was used as binder. The gas diffusion layer was made of carbon paper (10% GDL, 40% MPL, H2315T10AC) sourced from Freudenberg FCCT KG. Taking the anode preparation as an example, the ink was made by adding a small amount of de-ionized water into PTFE solution (20.4 mg) and mixing in a glass sample holder, followed by ultra-sonication for 15 min. The required amount of Pt/C catalyst (49.0 mg) and isopropanol (130.6 mg) were added to the aqueous PTFE solution, the suspension was

then placed in the ultrasonic bath for a further 30 min. The preparation was carried out at room temperature. The carbon paper was heated on a hot plate to maintain the temperature at 80 °C to 100 °C for good liquid evaporation. The ink was sprayed evenly onto the surface of the carbon paper using a Badger Model 100™ spray gun fed by N<sub>2</sub> gas. The Nafion 117 membrane was sandwiched between the cathode and the anode, and then hot pressed for 3 min at a pressure of 500 kg and temperature of 100 °C.

**Figure 6.** Schematic diagram of the fuel cell.



#### 4. Conclusions

It has been shown that an Al<sub>2</sub>O<sub>3</sub>-supported Si<sub>3</sub>N<sub>4</sub> membrane was capable of separating CO from a mixed stream of CO and H<sub>2</sub>. The separation phenomenon could be achieved via mixed chemisorption and physisorption functions. The separated CO was discharged from the bypass gas outlet so that the pressure in the cell remained the same as the surrounding atmosphere. A pore size of Si<sub>3</sub>N<sub>4</sub> could also block CO molecules and still allow H<sub>2</sub> to pass through the membrane. Since Si<sub>3</sub>N<sub>4</sub> has the advantages of being low cost and with ease of fabrication, it is probable that increasing the amount of Si<sub>3</sub>N<sub>4</sub> used or changing the fabrication method would further improve the efficiency of the Si<sub>3</sub>N<sub>4</sub> membrane to clean CO from a stream of H<sub>2</sub>.

#### Acknowledgments

We would like to thank EPSRC (ref. number RES05307354) for the financial support.

#### Conflicts of Interest

The authors declare no conflict of interest.

#### References

1. Lemons, R.A. Fuel cells for transportation. *J. Power Sources* **1990**, *29*, 251–264.
2. Iulianelli, A.; Longo, T.; Basile, A. Methanol steam reforming reaction in a Pd–Ag membrane reactor for CO-free hydrogen production. *Int. J. Hydrog. Energy* **2008**, *33*, 5583–5588.
3. Avgouropoulos, G.; Ioannides, T. CO tolerance of Pt and Rh catalysts: Effect of CO in the gas-phase oxidation of H<sub>2</sub> over Pt and Rh supported catalysts. *Appl. Catal. B Environ.* **2005**, *56*, 77–86.
4. Pereira, L.G.S.; Paganin, V.A.; Ticianelli, E.A. Investigation of the CO tolerance mechanism at several Pt-based bimetallic anode electrocatalysts in a PEM fuel cell. *Electrochim. Acta* **2009**, *54*, 1992–1998.
5. Tang, Y.; Zhang, H.; Zhong, H.; Xu, Z. *In-situ* investigation on the CO tolerance of carbon supported Pd–Pt electrocatalysts with low Pt content by electrochemical impedance spectroscopy. *Int. J. Hydrog. Energy* **2012**, *37*, 2129–2136.
6. Uchida, H.; Ozuka, H.; Watanabe, M. Electrochemical quartz crystal microbalance analysis of CO-tolerance at Pt–Fe alloy electrodes. *Electrochim. Acta* **2002**, *47*, 3629–3636.
7. Li, M.-Q.; Shao, Z.-G.; Scott, K. A high conductivity Cs<sub>2.5</sub>H<sub>0.5</sub>PMo<sub>12</sub>O<sub>40</sub>/polybenzimidazole (PBI)/H<sub>3</sub>PO<sub>4</sub> composite membrane for proton-exchange membrane fuel cells operating at high temperature. *J. Power Sources* **2008**, *183*, 69–75.
8. Mamlouk, M.; Scott, K. The effect of electrode parameters on performance of a phosphoric acid-doped PBI membrane fuel cell. *Int. J. Hydrog. Energy* **2010**, *35*, 784–793.
9. Mamlouk, M.; Scott, K. An investigation of Pt alloy oxygen reduction catalysts in phosphoric acid doped PBI fuel cells. *J. Power Sources* **2011**, *196*, 1084–1089.

10. Sousa, T.; Mamlouk, M.; Scott, K. A dynamic non-isothermal model of a laboratory intermediate temperature fuel cell using PBI doped phosphoric acid membranes. *Int. J. Hydrog. Energy* **2010**, *35*, 12065–12080.
11. Sousa, T.; Mamlouk, M.; Scott, K. An isothermal model of a laboratory intermediate temperature fuel cell using PBI doped phosphoric acid membranes. *Chem. Eng. Sci.* **2010**, *65*, 2513–2530.
12. Peters, R.; Düsterwald, H.G.; Höhle, B. Investigation of a methanol reformer concept considering the particular impact of dynamics and long-term stability for use in a fuel-cell-powered passenger car. *J. Power Sources* **2000**, *86*, 507–514.
13. Pettersson, L.J.; Westerholm, R. State of the art of multi-fuel reformers for fuel cell vehicles: Problem identification and research needs. *Int. J. Hydrog. Energy* **2001**, *26*, 243–264.
14. Cheng, F.; Clark, S.; Kelly, S.M.; Bradley, J.S.; Lefebvre, F. Preparation of mesoporous silicon nitride via a nonaqueous sol–gel route. *J. Am. Ceram. Soc.* **2004**, *87*, 1413–1417.
15. Cheng, F.; Kelly, S.M.; Clark, S.; Bradley, J.S.; Baumbach, M.; Schütze, A. Preparation and characterization of a supported Si<sub>3</sub>N<sub>4</sub> membrane via a non-aqueous sol–gel process. *J. Membr. Sci.* **2006**, *280*, 530–535.
16. Kuraoka, K.; Kubo, N.; Yazawa, T. Microporous silica xerogel membrane with high selectivity and high permeance for carbon dioxide separation. *J. Sol-Gel Sci. Technol.* **2000**, *19*, 515–518.
17. Mori, H.; Mase, S.; Yoshimura, N.; Hotta, T.; Ayama, K.; Tsubaki, J.I. Fabrication of supported Si<sub>3</sub>N<sub>4</sub> membranes using the pyrolysis of liquid polysilazane precursor. *J. Membr. Sci.* **1998**, *147*, 23–33.
18. Tong, H.D.; Jansen, H.V.; Gadgil, V.J.; Bostan, C.G.; Berenschot, E.; van Rijn, C.J.M.; Elwenspoek, M. Silicon nitride nanosieve membrane. *Nano Lett.* **2004**, *4*, 283–287.
19. Rovai, R.; Lehmann, C.W.; Bradley, J.S. Non-oxide sol–gel chemistry: Preparation from tris(dialkylamino)silazanes of a carbon-free, porous, silicon diimide gel. *Angew. Chem. Int. Ed.* **1999**, *38*, 2036–2038.
20. Mamlouk, M.; Scott, K. Analysis of high temperature polymer electrolyte membrane fuel cell electrodes using electrochemical impedance spectroscopy. *Electrochim. Acta* **2011**, *56*, 5493–5512.